

# Site-exchange of Li and M ions in silicate cathode materials $\text{Li}_2\text{MSiO}_4$ ( $M = \text{Mn, Fe, Co}$ and $\text{Ni}$ ): DFT calculations

Cite this: DOI: 10.1039/c3ta14885h

Lin Li,<sup>a</sup> Lin Zhu,<sup>a</sup> Lin-Han Xu,<sup>a</sup> Tai-Min Cheng,<sup>b</sup> Wei Wang,<sup>a</sup> Xiao Li<sup>a</sup> and Qiang-Tao Sui<sup>a</sup>

First principle calculations have been used to investigate the occurrence of site-exchange of Li and M ions and the effect of the site-exchange on Li extraction of silicate cathode materials  $\text{Li}_2\text{MSiO}_4$  ( $M = \text{Mn, Fe, Co}$  and  $\text{Ni}$ ). Total energy calculations suggest that Li (in the 4b site) and M (in the 2a site) ions become site-exchanged upon delithiation. This structural arrangement leads to significant cell expansion as two Li ions are extracted. Elastic property calculations indicate that the ductility of the fully delithiated  $\text{MSiO}_4$  is impaired, which is likely to induce structural collapse and rapid capacity attenuation during the charge–discharge cycles. Restraining the site-exchange or improving the ductility may be an effective way of developing high performance  $\text{Li}_2\text{MSiO}_4$  for Li-ion batteries.

Received 25th November 2013  
Accepted 2nd January 2014

DOI: 10.1039/c3ta14885h

[www.rsc.org/MaterialsA](http://www.rsc.org/MaterialsA)

## I. Introduction

As candidates for high performance cathode materials, lithium transition-metal silicates  $\text{Li}_2\text{FeSiO}_4$ ,  $\text{Li}_2\text{MnSiO}_4$  and their derived materials have been investigated experimentally and theoretically in previous studies.<sup>1–11</sup>  $\text{Li}_2\text{FeSiO}_4$  delivers excellent capacity retention, but exchanges only one Li ion per formula unit (FU).<sup>1–3</sup>  $\text{Li}_2\text{MnSiO}_4$  can easily exchange more than one Li ions in the first few charge–discharge cycles, but the capacity falls off drastically in the consecutive cycles.<sup>8,9</sup> *In situ* XRD and NMR measurements indicate that the structure of  $\text{Li}_2\text{MnSiO}_4$  is unstable upon delithiation, with a strong tendency to amorphize.<sup>10</sup>

The site-exchange (SE) of Li and M ions at 4b and 2a sites was experimentally observed in these materials.<sup>12,13</sup> Upon SE, the potential plateau of  $\text{Li}_2\text{FeSiO}_4$  shifts from 3.10 to 2.80 V.<sup>12</sup> Recent studies mainly focus on whether SE block Li ion diffusion.<sup>13–17</sup> As far as we know, the occurrence of SE, and the effects of this structural rearrangement on the overall electrochemical performance of these materials, such as the extraction of two Li ions and the cycle stabilities during the charge–discharge cycles, are not well understood. In this study, we present deintercalation potentials, total energies, and structural properties by DFT calculations to investigate systematically this structural rearrangement.

## II. Computational details

The DFT calculations were performed using the projector augmented wave (PAW)<sup>18</sup> scheme, as implemented in the VASP software package.<sup>19,20</sup> The exchange–correlation energies were approximated in the generalized gradient approximation (GGA) of Perdew, Burke and Ernzerhof (PBE).<sup>21</sup> To address on-site Coulomb interactions in the localized d electrons of transition-metal ions, additional Hubbard parameter correction was taken.<sup>22</sup> A *J* correction term of 1 eV was used, with a *U* value of 6 eV ( $M = \text{Mn, Co}$  and  $\text{Ni}$ ) and 5 eV ( $M = \text{Fe}$ ), in accordance with previous DFT+*U* investigations.<sup>7,23,24</sup>

The models of  $\text{Li}_4\text{M}_2\text{Si}_2\text{O}_8$  were constructed on the basis of  $\text{Li}_2\text{FeSiO}_4$  with the space group  $Pmn2_1$  – widely studied theoretically,<sup>9,25–27</sup> as seen in Fig. 1(A). The calculated most energetically favored SE configuration, in which M ions are as far as possible from each other, is given in Fig. 1(B). From the fully relaxed structure of  $\text{Li}_{4-x}\text{M}_2\text{Si}_2\text{O}_8$  ( $x = 0$  to 3), one Li ion was removed producing  $\text{Li}_{4-(x+1)}\text{M}_2\text{Si}_2\text{O}_8$ , which was also fully relaxed. The average lithium intercalation voltages were extracted from the total energies.<sup>29</sup> In order to determine the elastic constants we applied a set of normal and shear strains on crystals, and fitted the energy–strain curves of deformed crystals.

## III. Results and discussion

The calculated deintercalation potentials under the initial (INIT) state and the SE state are summarized in Fig. 2. Our results under the INIT state basically agree with the previous experimental and theoretical investigations.<sup>1–4,7,12,24</sup> Due to the stable  $3d^5$  configuration of  $\text{Fe}^{3+}$ ,  $\text{Li}_2\text{FeSiO}_4$  has the largest

<sup>a</sup>College of sciences, Northeastern University, Shenyang 110819, People's Republic of China<sup>b</sup>Department of Mathematics and Physics, Shenyang University of Chemical Technology, Shenyang 110142, People's Republic of China

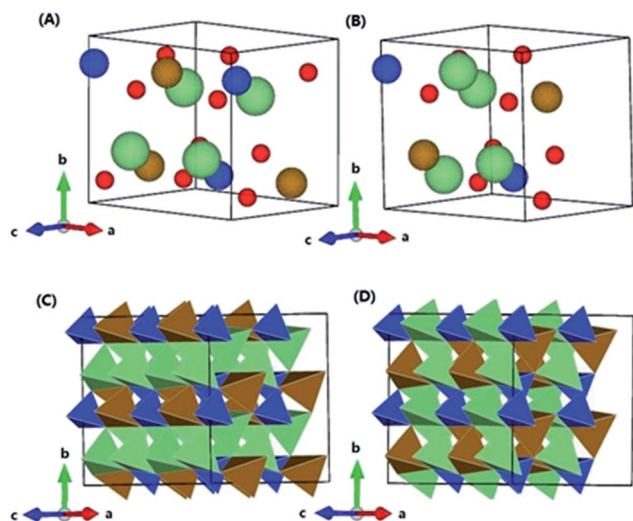


Fig. 1 The structure models of  $\text{Li}_2\text{MSiO}_4$  with the space group  $Pmn2_1$  symmetry (A). The energetically favored configuration of SE of Li and M ions (B) and their corresponding superlattices (C and D). The green, yellow, blue and red spheres represent Li, M, Si and O ions. The green, yellow and blue tetrahedra denote  $\text{LiO}_4$ ,  $\text{MO}_4$  and  $\text{SiO}_4$ . Structure drawing produced by using VESTA.<sup>28</sup>

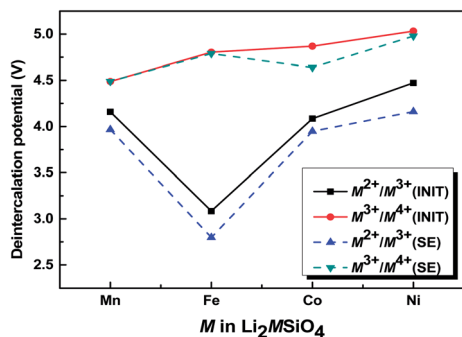


Fig. 2 Calculated deintercalation potentials of  $\text{Li}_2\text{MSiO}_4$  ( $M = \text{Mn, Fe, Co}$  and  $\text{Ni}$ ) under the INIT and the SE states.

potential step of 1.72 V between  $M^{2+}/M^{3+}$  and  $M^{3+}/M^{4+}$  couples. The step drops to 0.33 V for  $\text{Li}_2\text{MnSiO}_4$ . The SE phases generally have lower potentials than the INIT phases. The deintercalation potentials for extraction of the first Li in  $\text{Li}_2\text{FeSiO}_4$  under INIT and SE states are 3.08 and 2.80 V respectively, which corresponds to the experimentally observed plateau shift from 3.10 to 2.80 V upon structural rearrangement.<sup>12</sup>

We calculate the formation energies of  $\text{Li}_{2y}\text{MSiO}_4$  as

$$\Delta E(y) = E(y) - [yE(y=1) + (1-y)E(y=0)]$$

where  $E(y)$  is the total energy of the structure with  $2y$  Li ions, and  $E(y=1)$  and  $E(y=0)$  are the total energies of  $\text{Li}_2\text{MSiO}_4$  and fully delithiated  $\text{MSiO}_4$ , respectively. Negative formation energy suggests that a compound with the given Li concentration is energetically stable, while positive formation energy means occurrence of phase separation. In GGA calculation of ref. 10, the formation energies of  $\text{Li}_2\text{MnSiO}_4$  are positive in the whole

concentration range. Phase separation of  $\text{LiMnSiO}_4$  into  $\text{Li}_2\text{MnSiO}_4$  and  $\text{MnSiO}_4$  was ascribed to the amorphism during the delithiation process. In our GGA+ $U$  calculation  $\text{LiMnSiO}_4$  has the highest formation energies among these materials under both INIT and SE states, whereas it does not show any sign of phase separation. The amorphism of  $\text{Li}_2\text{MnSiO}_4$  upon delithiation seems to be irrelevant to the phase separation (Fig. 3).

The relative total energies between SE and INIT  $\text{Li}_{2-x}\text{MSiO}_4$  are given as a function of Li concentration in Fig. 4. In most cases (except Co),  $\text{Li}_2\text{MSiO}_4$  energetically prefers the INIT state, consistent with the structural data obtained in experiments.<sup>1,5,6</sup> The SE of Li and Co can be directly observed from the XRD profile of  $\text{Li}_2\text{CoSiO}_4$  without delithiation.<sup>31</sup> Upon delithiation the SE state plays a dominant role, leading to the change in the Li : M ratio at the 4b site. Generally this structural rearrangement in  $\text{Li}_2\text{MSiO}_4$  during delithiation is a phase transition to a more stable structure and causes slight decrease of the potential plateau.

As M ions are oxidized from  $M^{2+}$  to a higher valency the M–O bond contracts, due to the so-called rehybridization shift.<sup>32–35</sup> The bond lengths of M–O decrease with Li extraction, whereas the cell volumes in the INIT state increase except for  $M = \text{Mn}$ , as

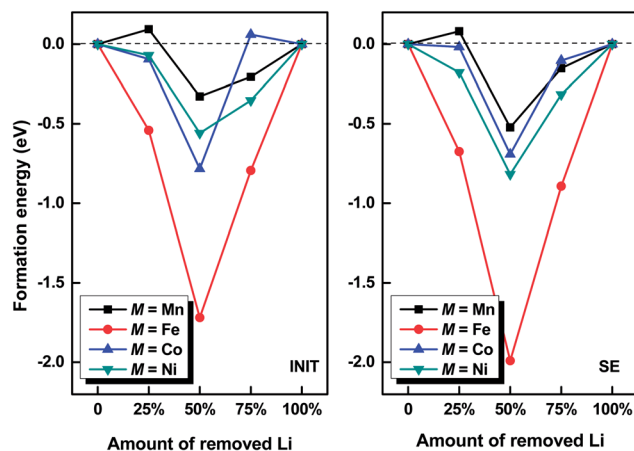


Fig. 3 Formation energies of  $\text{Li}_{2-2x}\text{MSiO}_4$  ( $x = 0, 50\%, 100\%$ ) under the INIT and the SE states as a function of Li concentration.

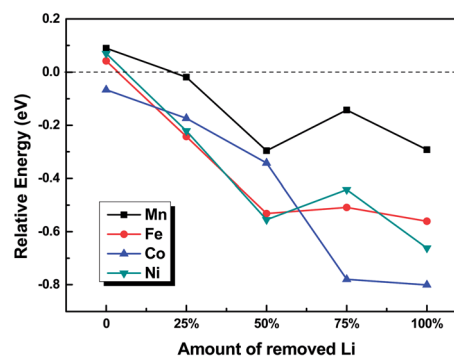


Fig. 4 Energy differences between the SE and the INIT  $\text{Li}_{2-2x}\text{MSiO}_4$  ( $x = 0, 50\%, 100\%$ ) as a function of Li concentration.

seen in Fig. 5. With one Li ion extraction, the  $\text{LiMSiO}_4$  cells expand by less than 2%. The fully delithiated  $\text{NiSiO}_4$  cell expands by 9%, and  $\text{FeSiO}_4$  and  $\text{CoSiO}_4$  cells expand by 5%. By comparison with  $\text{Li}_2\text{MnSiO}_4$ ,  $\text{LiMnSiO}_4$  and  $\text{MnSiO}_4$  cells contract by 2% and 5%, respectively. In the energetically favored SE state,  $\text{LiMSiO}_4$  ( $M = \text{Fe}, \text{Co}$  and  $\text{Ni}$ ) cells expand by about 2%, slightly higher than the INIT cells. The SE  $\text{MSiO}_4$  cells expand significantly, by more than 22%. The SE cell almost stays at the same level for  $\text{LiMnSiO}_4$  and expands by 7% for  $\text{MnSiO}_4$ .

From Fig. 6 we find that the expansion of most of the INIT  $\text{Li}_2\text{MSiO}_4$  cells (except  $M = \text{Mn}$ ) is mainly contributed by the increase of the cell parameters  $b$  and  $c$ . Li extraction weakens the attraction of adjacent two  $\text{MSiO}_4$  layers, and the cell expands along the  $b$ -axis as a result (see Fig. 1(C)). A corrugated chain along the  $c$ -axis is formed by the  $\text{MO}_4$  and  $\text{SiO}_4$  tetrahedra sharing one oxygen atom. The chain becomes less corrugated with Li extraction, leading to the expansion along the  $c$ -axis. In the case of  $M = \text{Mn}$ , the flattening of the tetrahedra chains is less pronounced, which does not compensate the contraction of the Mn–O bond.

The SE structure of  $\text{Li}_2\text{MSiO}_4$  can be described as being built up of chains of  $\text{SiO}_4$  and  $\text{MO}_4$  tetrahedra along the  $b$ -axis and linked by  $\text{LiO}_4$  tetrahedra along the  $a$ - and  $c$ -axes (see Fig. 1(D)). For  $M = \text{Fe}, \text{Co}$  and  $\text{Ni}$ , Li extraction leads to the simultaneous increase of the parameters  $a$  and  $c$ , which is the major driving force for the significant cell expansion in the SE state. In addition, the SE cells approximately maintain the orthorhombic lattices during delithiation, while the INIT structure tends to be monoclinic which alleviate the cell expansion in the INIT state. The SE  $\text{MnSiO}_4$  cell contracts along the  $c$ -axis, which is similar to that of the INIT cell, leading to the moderate cell expansion of 7%.

$\text{Li}_2\text{MSiO}_4$  can be classified into two groups,  $M = \text{Fe}, \text{Co}$  and  $\text{Ni}$  and  $M = \text{Mn}$ , according to the degree of cell expansion during delithiation. In order to investigate the structural stability of the energetically favored delithiated SE cells we calculate the elastic constants of delithiated  $\text{LiFeSiO}_4$ ,  $\text{FeSiO}_4$ ,  $\text{LiMnSiO}_4$  and  $\text{MnSiO}_4$ , as listed in Table 1. The delithiated

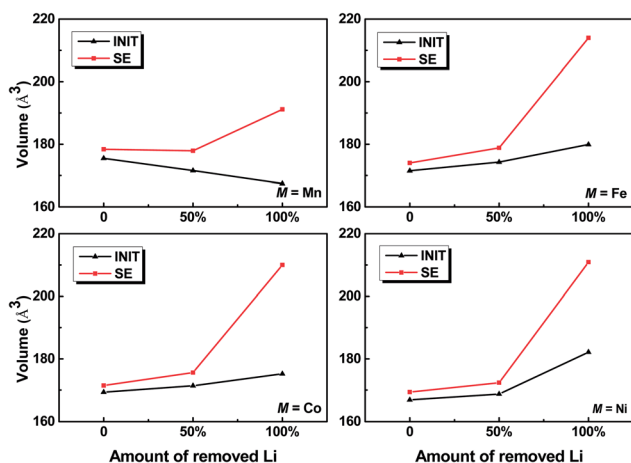


Fig. 5 Cell volumes of  $\text{Li}_{2-2x}\text{MSiO}_4$  ( $x = 0, 50\%, 100\%$ ) under the INIT and the SE states as a function of Li concentration.

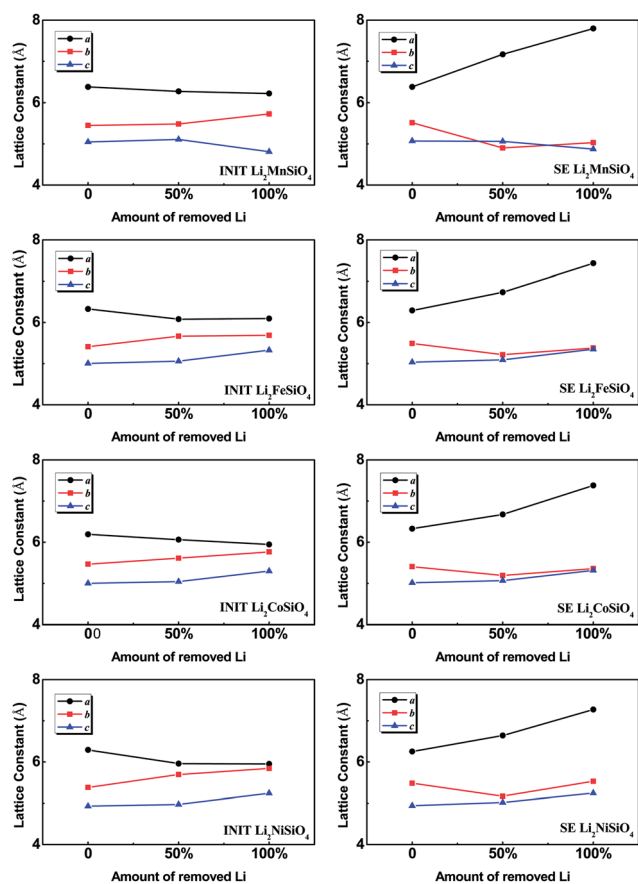


Fig. 6 Variation of lattice parameters  $a$ ,  $b$  and  $c$  of  $\text{Li}_{2-2x}\text{MSiO}_4$  ( $x = 0, 50\%, 100\%$ ) under the INIT (in the left panel) and the SE (in the right panel) states as a function of Li concentration.

cells, which belong to the triclinic system, have 21 independent elastic constants. The mechanical stability criterion is given as the eigenvalues of the elastic stiffness matrix are larger than zero. A parameter  $B/G$  is also introduced, in which  $B$  indicates the bulk modulus and  $G$  represents the shear modulus. The bulk and shear moduli are calculated from the Voigt–Reuss–Hill approximations.<sup>36–38</sup> The high (low)  $B/G$  value is associated with ductility (brittleness), and the critical value which separates ductile and brittle materials is 1.75.<sup>39</sup> The calculated four groups of eigenvalues meet the mechanical stability criterion. The calculated  $B/G$  values of  $\text{LiFeSiO}_4$  and  $\text{LiMnSiO}_4$  are 1.76 and 1.90 respectively, indicating that they are ductile. However, the values are 0.74 and 1.10 respectively for  $\text{FeSiO}_4$  and  $\text{MnSiO}_4$ . The fully delithiated materials are brittle. With the extraction and the insertion of Li ions, the cell expands and contracts continuously and is likely to collapse, it is the reason for the formation of the amorphous-like region and the drastic fade in the capacity of  $\text{Li}_2\text{MnSiO}_4$  after the first few charge–discharge cycles.

Due to the higher deintercalation potential of 4.79 V in SE  $\text{Li}_2\text{FeSiO}_4$ , the extraction of the second Li is difficult. As one Li is extracted, the volume change of the SE cell is only 2.8%. Hence  $\text{Li}_2\text{FeSiO}_4$  shows excellent capacity retention. The  $B/G$  value of  $\text{FeSiO}_4$  is far less than that of  $\text{MnSiO}_4$  and the critical value is

**Table 1** Calculated elastic stiffness matrices (GPa) of  $\text{LiMnSiO}_4$ ,  $\text{MnSiO}_4$ ,  $\text{LiFeSiO}_4$  and  $\text{FeSiO}_4$ , and the corresponding eigenvalues and  $B/G$  values

$c_{ij}$	Eigenvalue						$B/G$
<b><math>\text{LiMnSiO}_4</math></b>							
108.87	45.02	45.86	-0.23	1.67	-0.49	19.64	1.92
45.02	66.78	22.89	-0.37	-4.13	-0.21	28.29	
45.86	22.89	85.42	-0.28	-8.34	-0.24	37.29	
-0.23	-0.37	-0.28	19.68	-0.15	-0.72	40.84	
1.67	-4.13	-8.34	-0.15	33.73	-0.29	56.73	
-0.49	-0.21	-0.24	-0.72	-0.29	37.27	168.97	
<b><math>\text{MnSiO}_4</math></b>							
38.28	8.67	3.46	-0.17	-0.59	0.08	3.98	1.24
8.67	25.14	5.38	2.31	1.46	2.59	13.73	
3.46	5.38	24.83	0.19	-4.50	0.05	15.79	
-0.17	2.31	0.19	4.30	0.2	0.77	22.5	
-0.59	1.46	-4.50	0.20	19.08	0.13	26.69	
0.08	2.59	0.05	0.77	0.13	15.37	44.32	
<b><math>\text{LiFeSiO}_4</math></b>							
87.45	42.44	31.10	0.05	-0.43	0.06	23.94	1.76
42.44	108.28	32.09	-0.01	-0.29	-0.10	36.48	
31.10	32.09	99.32	0.12	-0.49	0.05	38.33	
0.05	-0.01	0.12	23.94	0.06	-0.03	53.25	
-0.43	-0.29	-0.49	0.06	36.52	0.25	72.10	
0.06	-0.10	0.05	-0.03	0.25	38.30	169.70	
<b><math>\text{FeSiO}_4</math></b>							
22.45	5.49	3.29	0.05	-0.17	-0.11	5.8272	1.02
5.49	21.80	4.64	0.33	0.34	0.12	11.1255	
3.29	4.64	28.56	0.18	-0.13	-0.80	16.4823	
0.05	0.33	0.18	6.24	-0.05	1.42	22.5196	
-0.17	0.34	-0.13	-0.05	22.66	0.22	22.7897	
-0.11	0.12	-0.80	1.42	0.22	10.77	33.7508	

1.75. If the extraction of two Li ions is possible within the limit of electrolyte, the significant cell expansion of  $\text{FeSiO}_4$  will produce even worse electrochemical performance. Considering the higher deintercalation potential of the second Li ion in  $\text{Li}_2\text{FeSiO}_4$  beyond the limit of most electrolytes, the structural collapse of  $\text{FeSiO}_4$  cannot be confirmed directly by experiment. The cell expansions of  $\text{Li}_2\text{CoSiO}_4$  and  $\text{Li}_2\text{NiSiO}_4$  during the delithiation process approximate to that of  $\text{Li}_2\text{FeSiO}_4$ . We deduce that the delithiated phases of these three materials have similar  $B/G$  values. The calculated deintercalation potential for the second Li in  $\text{Li}_2\text{CoSiO}_4$  is 4.61 V, smaller than 4.79 V of  $\text{Li}_2\text{FeSiO}_4$ . In a potential range of 3.0 to 4.6 V, there is a large irreversible capacity during the first cycle, about 1.4 Li per FU is extracted and only 0.46 Li per FU can be inserted back.<sup>31</sup>

Our calculated results suggest that the SE effects of  $\text{Li}_2\text{MSiO}_4$  should be emphasized in future theoretical and experimental studies. As the SE of Li and M ions induces significant cell expansion, restraining SE may directly reduce the probability of structural collapse during the charge–discharge cycles. In addition, promoting ductility is another effective way to improve the electrochemical performance of the silicate cathode materials. Due to the lower deintercalation potential, smaller cell expansion and higher  $B/G$  value, modified

$\text{Li}_2\text{MnSiO}_4$  is expected to become one of the most promising candidates for silicate cathode materials.

## IV. Conclusion

The site-exchange of Li and M ions on the electrochemical performance of silicate cathode materials  $\text{Li}_2\text{MSiO}_4$  ( $M = \text{Mn}, \text{Fe}, \text{Co}$  and  $\text{Ni}$ ) has been investigated by DFT calculations. The site-exchange is a phase transition to a more stable structure during the delithiation process. In the energetically favored site-exchange state fully delithiated  $\text{MSiO}_4$  become brittle, which damages the cycle stability, due to the significant cell expansion. As  $\text{MnSiO}_4$  has a slightly moderate cell expansion and a relatively higher  $B/G$  value. The reversible extraction and insertion of two Li ions in modified  $\text{Li}_2\text{MnSiO}_4$  is easy to perform among these four materials.

## Acknowledgements

The authors thank the National Natural Science Foundation of China (NNSFC) for financial support (Grants no. 11374215).

## References

- 1 A. Nytén, A. Abouimrane, M. Armand, T. Gustafsson and J. O. Thomas, *Electrochem. Commun.*, 2005, **7**, 156.
- 2 R. Dominko, M. Bele, M. Gabersček, A. Meden, M. Remškar and J. Jamnik, *Electrochem. Commun.*, 2006, **8**, 217.
- 3 R. Dominko, D. E. Conte, D. Hanzel, M. Gaberscek and J. Jamnik, *J. Power Sources*, 2008, **178**, 842.
- 4 R. Dominko, M. Bele, A. Kokalj, M. Gaberscek and J. Jamnik, *J. Power Sources*, 2007, **174**, 457.
- 5 C. Deng, S. Zhangb and S. Y. Yang, *J. Alloys Compd.*, 2009, **487**, L18.
- 6 C. Deng, S. Zhang, B. L. Fu, S. Y. Yang and L. Ma, *Mater. Chem. Phys.*, 2010, **120**, 14.
- 7 M. E. Arroyo-de Dompablo, M. Armand, J. M. Tarascon and U. Amador, *Electrochem. Commun.*, 2006, **8**, 1292.
- 8 V. Aravindan, K. Karthikeyan, S. Ravi, S. Amaresh, W. S. Kim and Y. S. Lee, *J. Mater. Chem.*, 2010, **20**, 7340.
- 9 Z. L. Gong, Y. X. Li and Y. Yang, *Electrochem. Solid-State Lett.*, 2006, **9**, A542.
- 10 A. Kokalj, R. Dominko, G. Mali, A. Meden, M. Gaberscek and J. Jamnik, *Chem. Mater.*, 2007, **19**, 3633.
- 11 D. Su, H. Ahn and G. Wang, *Appl. Phys. Lett.*, 2011, **99**, 141909.
- 12 A. Nytén, S. Kamali, L. Häggström, T. Gustafsson and J. O. Thomas, *J. Mater. Chem.*, 2006, **16**, 2266.
- 13 I. Belharouak, A. Abouimrane and K. Amine, *J. Phys. Chem. C*, 2009, **113**, 20733.
- 14 A. Rougier, P. Gravereau and C. Delmas, *J. Electrochem. Soc.*, 1996, **143**, 1168.
- 15 N. Kuganathan and M. S. Islam, *Chem. Mater.*, 2009, **21**, 5196.
- 16 G. R. Gardiner and M. S. Islam, *Chem. Mater.*, 2010, **22**, 1242.
- 17 A. Liivat and J. O. Thomas, *Solid State Ionics*, 2011, **192**, 58.
- 18 P. E. Blöchl, *Phys. Rev. B: Condens. Matter Mater. Phys.*, 1994, **50**, 17953.

- 1 19 G. Kresse and J. Joubert, *Phys. Rev. B: Condens. Matter Mater. Phys.*, 1996, **54**, 11169.
- 20 G. Kresse and J. Furthmuller, *Comput. Mater. Sci.*, 1996, **6**, 15.
- 5 21 J. Perdew, K. Burke and M. Ernzerhof, *Phys. Rev. Lett.*, 1996, **77**, 3865.
- 22 S. L. Dudarev, G. A. Botton, S. Y. Savrasov, C. J. Humphreys and A. P. Sutton, *Phys. Rev. B: Condens. Matter Mater. Phys.*, 1998, **57**, 1505.
- 10 23 L. Wang, T. Maxisch and G. Ceder, *Phys. Rev. B: Condens. Matter Mater. Phys.*, 2006, **73**, 195107.
- 24 Y. Li, X. Cheng and Y. Zhang, *J. Electrochem. Soc.*, 2012, **159**, A69.
- 15 25 A. Kokalj, R. Dominko, G. Mali, A. Meden, M. Gaberscek and J. Jamnik, *Chem. Mater.*, 2007, **19**, 3633.
- 26 P. Larsson, R. Ahuja, A. Nytén and J. O. Thomas, *Electrochem. Commun.*, 2006, **8**, 797.
- 27 S. Q. Wu, Z. Z. Zhu, Y. Yang and Z. F. Hou, *Comput. Mater. Sci.*, 2009, **44**, 1243.
- 20 28 K. Momma and F. Izumi, *J. Appl. Crystallogr.*, 2011, **44**, 1272.
- 29 M. K. Aydinol, A. F. Kohan, G. Ceder, K. Cho and J. Joannopoulos, *Phys. Rev. B: Condens. Matter Mater. Phys.*, 1997, **56**, 1354.
- 30 G. Henkelman and H. Jonsson, *J. Chem. Phys.*, 2000, **113**, 9978.
- 31 A. R. Armstrong, C. Lyness, M. Ménétrier and P. G. Bruce, *Chem. Mater.*, 2010, **22**, 1892.
- 32 F. Zhou, M. Cococcioni, K. Kang and G. Ceder, *Electrochem. Commun.*, 2004, **6**, 1144.
- 33 C. A. Marianetti, G. Kotliar and G. Ceder, *Phys. Rev. Lett.*, 2004, **92**, 196405.
- 34 J. Graetz, A. Hightower, C. C. Ahn, R. Yazami, P. Rez and B. Fultz, *J. Phys. Chem. B*, 2002, **106**, 1286.
- 35 G. Zhong, Y. Li, P. Yan, Z. Liu, M. Xie and H. Lin, *J. Phys. Chem. C*, 2010, **114**, 3693.
- 15 36 W. Voigt, *Lehrbuch der Kristallphysik*, ed. Teubner, Leipzig, 1928.
- 37 A. Reuss, *Z. Angew. Math. Mech.*, 1929, **9**, 49.
- 38 R. Hill, *Proc. Phys. Soc., London*, 1952, **65**, 350.
- 20 39 S. F. Pugh, *Philos. Mag.*, 1954, **45**, 823.
- 25
- 30
- 35
- 40
- 45
- 50
- 55